Hindawi Publishing Corporation
Mathematical Problems in Engineering
Volume 2010, Article ID 768256, 13 pages
doi:10.1155/2010/768256

Research Article

The Comparative Study of Vibration Control of Flexible Structure Using Smart Materials

Juntao Fei,[1,2] Yunmei Fang,[3] and Chunyan Yan[3]

[1] *Jiangsu Key Laboratory of Power Transmission and Distribution Equipment Technology, Jiangsu 213022, China*
[2] *College of Computer and Information, Hohai University, Changzhou 213022, China*
[3] *College of Mechanical and Electronics Engineering, Hohai University, Changzhou 213022, China*

Correspondence should be addressed to Juntao Fei, jtfei@yahoo.com

Received 24 June 2010; Revised 26 October 2010; Accepted 28 October 2010

Academic Editor: Alexander P. Seyranian

Considerable attention has been devoted to active vibration control using intelligent materials as PZT actuators. This paper presents results on active control schemes for vibration suppression of flexible steel cantilever beam with bonded piezoelectric actuators. The PZT patches are surface bonded near the fixed end of flexible steel cantilever beam. The dynamic model of the flexible steel cantilever beam is derived. Active vibration control methods: optimal PID control, strain rate feedback control (SRF), and positive position feedback control (PPF) are investigated and implemented using xPC Target real-time system. Experimental results demonstrate that the SRF and PPF controls have better performance in suppressing the vibration of cantilever steel beam than the optimal PID control.

1. Introduction

Actuators from piezoceramic materials have wide application ranging from active vibration control to nanoscale positioning tasks. This is due to their high-frequency response behavior and essentially infinite resolution. Because piezoelectric ceramic materials have mechanical simplicity, small volume, light weight, large useful bandwidth, efficient conversion between electrical energy and mechanical energy, and easy integration with various metallic and composite structures, smart structures with surface-mounted or embedded piezoelectric ceramic patches have received much attention in vibration control of structures in recent years. Within the last two decades, much attention has been focused on active control of structures to suppress their structural vibrations. Active control methods can be used to damp out undesirable structural vibrations. Strain rate feedback (SRF) control is used for active

damping of a flexible space structure by Newman [1]. Crawley and de Luis [2] proposed piezoelectric materials to be built in laminated beams. Fanson and Caughey [3] carried out feedback control to suppress structural vibration with segmented piezoelectric actuators and sensors. Positive position feedback (PPF) [4–7] is applied by feeding the structural position coordinate directly to the compensator, and the product of the compensator and a scalar gain positively back to the structure. The model derivation for a vibrating beam is described in many texts. Choi and Lee [8] presented the derivation for the modeling of a beam with a piezoceramic actuator affixed near the base. Many approximate models have been developed to predict the behavior of flexible beams incorporating PZT actuators [9–11]. Adaptive sliding model controller with sliding mode compensator has been developed in [12]. Active vibration suppression of a flexible steel cantilever beam using smart materials is proposed in [13]. Jiang et al. [14] designed a robust adaptive integral variable structure attitude controller with application to flexible spacecraft. Qiu et al. [15] developed a discrete-time sliding mode control to suppress vibration of the flexible plate.

In this paper, the dynamic modeling and the active vibration control scheme SRF and PPF control for the vibration suppression of steel cantilever beam are investigated and compared. The contribution of this paper is that the vibration control of flexible structure using PPF and SRF are implemented with X-PC Target real-time control system. This paper is organized as follows. In Section 2, the dynamical model of flexible structure using finite element model is derived. In Section 3, vibration controls such as PPF and SRF-controllers are described. Experiment results are given and analyzed in detail in Section 4. Conclusion is summarized in Section 5.

2. Dynamical Model

The flexible beam is modeled using the finite element method. The structure is divided into elements that are connected at a finite number of points, called nodes. The motion of the points in the element is defined in terms of nodal displacement and interpolation functions. Therefore, first the stiffness and mass matrices of the elements are analyzed. The elements are assembled to determine the stiffness and mass matrices of the structure. The first three modes might be enough to model the flexible beam if the bandwidth of the actuator is less than the frequency of the third mode. Similarly, if the band width of the sensor is less than the third modes, higher vibration modes will not be seen from the sensor output. In addition, a low-pass filter or a spillover filter could be used to reduce the effect of the unmodeled modes in the experiment and simulation. Therefore, no more than three lowest modes are significant in the response of the appendage and thus would be considered in the simulations. In this section, six elements were used to characterize the structure. The flexible arm was divided into six elements and motion was considered to be inplane bending based on the cantilever action. The system consists of 6 elements and 7 nodes (as shown in Figure 1). PZT sensors and actuators are attached to the element 2 of the beam. The PZTs add to the beam's stiffness and hence increase the fundamental frequency.

The following are equations and procedure in finite element modeling. The general relationship for the electromechanical coupling is given by

$$\begin{Bmatrix} D_3 \\ S_1 \end{Bmatrix} = \begin{bmatrix} \varepsilon_3^T & d_{31} \\ d_{31} & s_{11}^E \end{bmatrix} \begin{Bmatrix} E_3 \\ T_1 \end{Bmatrix}, \tag{2.1}$$

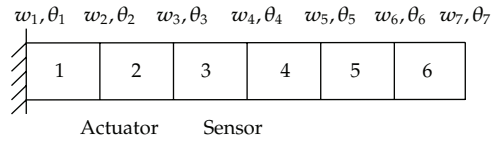

Figure 1: Elemental model of the flexible beam.

where D is the displacement, S is the strain, E is the electric field, T is the stress, s is the compliance and d is the piezoelectric constant. The subscripts are tensor notation where the 1- and 2-axes are arbitrary in the plane perpendicular to the 3-axis poling direction of the piezoelectric material. Using the fact that the elastic constant for piezoceramic material, s, is the inverse of its Young's modulus E_p, (2.2) can be written as

$$\begin{Bmatrix} D_3 \\ T_1 \end{Bmatrix} = \begin{bmatrix} \varepsilon_3^T - d_{31}^2 E_p & d_{31} E_p \\ -d_{31} E_p & E_p \end{bmatrix} \begin{Bmatrix} E_3 \\ S_1 \end{Bmatrix}, \tag{2.2}$$

where ε_3 is the permittivity of piezoelectric material, E_p is the elastic modulus, d_{31} is the piezoelectric charge coefficient, E_3 is the applied field intensity.

The general form of the energy equation is

$$-U = \frac{1}{2}\gamma e^2 - q^T B e - \frac{1}{2} q^T K q, \tag{2.3}$$

where

$$\begin{aligned} \gamma &= \frac{W_p h}{t_p}\left(\varepsilon_3^T - d_{31}^2 E_p\right), \quad e = t_p E_3, \\ B^T &= \begin{bmatrix} b_1 & b_2 & b_3 & b_4 \end{bmatrix}, \quad b_1 = b_3 = 0, \\ b_2 &= -b_4 = -d_{31} E_p W_p \left(\varsigma + \frac{t_p}{2}\right), \end{aligned} \tag{2.4}$$

where $K = k_b + k_p$, k_b is stiffness matrix for the structure, k_p is stiffness matrix for the piezoceramic, q is the generalized coordinate and B is the electromechanical coupling term which represents the conversion of electrical voltage to mechanical displacement, W_p as width of the piezoceramic wafer, t_p is thickness of piezoceramic, ς is half of the thickness of beam.

The total kinetic energy is given by

$$T = \frac{1}{2}\dot{q}^T M \dot{q}, \tag{2.5}$$

where $M = M_b + M_p$, and M_b is mass matrix for beam, M_p is mass matrix for PZT.

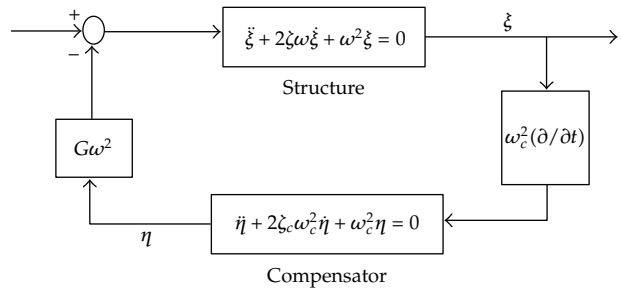

Figure 2: Block diagram of SRF-controller.

The Lagrangian function L is

$$L = T - U = \frac{1}{2}\dot{q}^T M_p \dot{q} + \frac{1}{2}\gamma e^2 - q^T B e - \frac{1}{2} q^T K q. \tag{2.6}$$

The Lagrangian equation is

$$\frac{d}{dt}\left(\frac{\partial L}{\partial \dot{q}_k}\right) - \frac{\partial L}{\partial q_k} = 0. \tag{2.7}$$

The equation for the actuator is

$$M\ddot{q} + Kq = -Be_a, \tag{2.8}$$

where $M = M_b + M_p$ and e_a is applied voltage.

The piezoceramic sensor voltage output is $\gamma e_s = B^T q$. We have considered only an element. The equation for the global form is determined by combining the equations. From the FEM modal analysis, there are variations of natural frequencies of beams with the bonded actuators and sensor. Numerical results show that the bonded actuators and sensors lead to increase in natural frequencies. The dynamic effects of mass and stiffness of the piezoelectric patch are considered in the model procedure.

3. Vibration Control

For this research two vibration suppression methods are used, strain rate feedback control and positive position feedback control.

3.1. Strain Rate Feedback (SRF) Control

Strain rate feedback (SRF) control is used for active damping of a flexible space structure. Using SRF, the structural velocity coordinate is fed back to the compensator, and the compensator position coordinate multiplied by a negative gain is fed back to the structure. SRF has a wider active damping region and can stabilize more than one mode given a sufficient bandwidth. In this research, the SRF is designed to control the vibration of the

first mode. Experimental results demonstrate that the SRF method is effective in actively increasing damping of the flexible beam with the PZT actuator. The SRF model can be presented with the following equations:

$$\ddot{\xi} + 2\zeta w\dot{\xi} + w^2\xi = -Gw^2\eta, \tag{3.1}$$

$$\ddot{\eta} + 2\zeta_C w_C\dot{\eta} + w_C\eta = w_C^2\dot{\xi}. \tag{3.2}$$

Figure 2 shows SRF block diagram, where ξ is a modal coordinate of structure displacement, ζ is the damping ratio of the structure, ω is the natural frequency of the structure, G is the feedback gain, η is the compensator coordinate, ζ_c is the damping ratio of the compensator, ω_c is the natural frequency of the compensator. SRF control is implemented by feeding the velocity coordinate to the compensator. The position coordinate of the compensator is then fed back with a negative gain to the structure. To illustrate the operation of a SRF-controller, assume a single degree-of-freedom vibration of the beam in the form of $\xi(t) = \alpha e^{i\omega t}$, and output of compensator at steady state is

$$\eta(t) = \beta e^{i(\omega t + 0.5\pi - \phi)}, \tag{3.3}$$

where phase angle ϕ is given by

$$\phi = \tan^{-1}\left(2\zeta_C \frac{\omega/\omega_C}{\left(1 - \omega^2/\omega_C^2\right)}\right), \tag{3.4}$$

and the magnitude β is given by

$$\beta = \frac{\alpha}{\sqrt{\left(1 - \omega^2/\omega_C^2\right)^2 + \left(2\zeta_C(\omega/\omega_C)\right)^2}}. \tag{3.5}$$

When the natural frequency of structure is much lower than the compensator natural frequency the phase angle ϕ approaches zero.

Substituting (3.3) with $\phi = 0$ into (3.1) results in

$$\ddot{\xi} + \left(2\zeta w + G\beta\omega\right)\dot{\xi} + w^2\xi = 0. \tag{3.6}$$

It is clear from (3.5) that the SRF compensator at this time results in an increase in the damping ratio, which is called active damping. When the compensator and the structure have the same natural frequency, the phase angle ϕ approaches $\pi/2$. After substituting (3.3) with $\phi = \pi/2$ into (3.1), the structural equation becomes

$$\ddot{\xi} + 2\zeta w\dot{\xi} + \left(w^2 + G\beta\omega^2\right)\xi = 0. \tag{3.7}$$

Equation (3.7) shows that the SRF compensator causes an increase in the stiffness term, which is called active stiffness. When the compensator frequency is much lower than that of the structure, the phase angle ϕ approaches π.

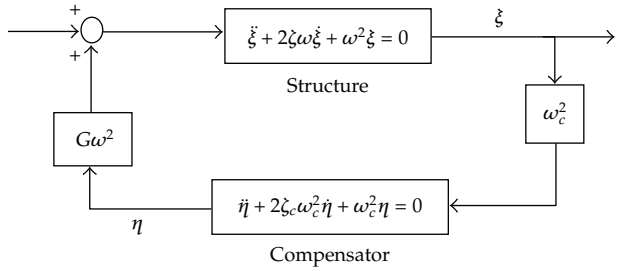

Figure 3: Block diagram of PPF controller.

Substituting (3.3) with $\phi = \pi$ into (3.1) results in equation

$$\ddot{\xi} + (2\zeta w - G\beta\omega)\dot{\xi} + w^2\xi = 0. \tag{3.8}$$

It is clear from (3.8) that the effect of the SRF compensator is a decrease in the damping term, which is referred to as active negative damping. Thus, in implementing SRF, the compensator should be designed so the targeted frequencies are below the compensator frequencies. SRF has a much wider active damping frequency region, which gives a designer some flexibility. As long as the compensator frequency is greater than the structural frequency, a certain amount of damping will be provided.

3.2. Positive Position Feedback Control

Positive Position Feedback (PPF) control was first proposed by Goh and Caughey for he collocated sensors and actuators. Later on Fanson and Caughey demonstrated PPF control in large space structures. The PPF control is applied by feeding the structural position coordinate directly to the compensator and the product of the compensator and a scalar gain positively back to the structure. PPF offers quick damping for a particular mode provided that the modal characteristics are known. The scalar equations governing the vibration of the structure in a single mode and the PPF controller are given as follows:

$$\begin{aligned} \ddot{\xi} + 2\delta\omega\dot{\xi} + \omega^2\zeta &= G\omega^2\eta, \\ \ddot{\eta} + 2\delta_c\omega_c^2\dot{\eta} + \omega_c^2 &= \omega_c^2\zeta, \end{aligned} \tag{3.9}$$

where ζ is a modal coordinate of structure displacement, δ is the damping ratio of the structure, ω is the natural frequency of the structure, G is the feedback gain, η is the compensator coordinate, δ_c is the damping ratio of the compensator, ω_c is the natural frequency of the compensator. The PPF control is illustrated in the block diagram as shown in Figure 3. In PPF control, ω_c should be closely matched to the natural frequency ω of the structure in order to achieve maximum damping.

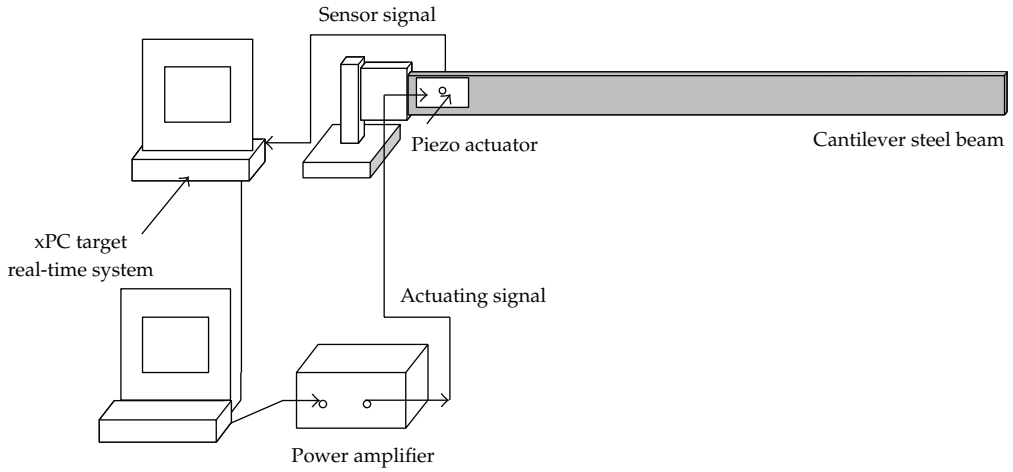

Figure 4: Schematic diagram of real-time experimental setup for active control.

4. Experiment Results

4.1. Experiment Setup

The control objective is to show the effectiveness of various vibration suppression strategies for a cantilever steel beam by using smart actuators. To achieve this control objective an experiment is set up. The steel beam is cantilevered at one end and PZT actuators are bonded to the surface of beam. One patch (model no PZTQP-20W) is bonded on one side of the beam near the base. A strain gage (EA-ϕ5-125UN-350) is affixed to the beam as sensor. Figure 4 depicts the real situation experiment of a flexible cantilever steel beam. These PZT patches are used as actuators to excite the beam and to enable active control of the beam vibration. The strain gage is used to detect the sensor signal for the feedback of the signal in the active control algorithms.

In general research, the control algorithm is designed in the MATLAB/SIMULINK and then downloaded to the xPC Target digital signal processor for implementation. The xPC-Target digital data acquisition system is used to capture the experimental data. The target and host computer are used in the experiment. The input signals to the PZT actuators in the experiment are amplified using voltage amplifier whose signals drive the PZT actuators and are used to excite the beam. The sensor signals from the beam are captured using strain gage and used for the feedback control.

In order to experimentally identify the dominant modes of the beam at which the controller should target, open-loop testing was performed The beam was excited by manually tapping at its free end and the data was record in the xPC-target system. Because system errors and environmental factors may influence the sensor measurements, the sensors calibration is required before the experiment. The amplitude vibrates around -0.448 under free conditions, so all the acquisition data should be compensated with -0.448 as the sensors calibration. To determine the first natural frequency w_n and the damping coefficient ζ, ten pulses were selected. The damping coefficient is $\zeta = (1/2\pi(10)) \ln(A_1/A_{10}) = 0.45\%$, where, A_1 and A_{10} are the amplitudes of the 1st peak and 10th peak respectively. It can be derived that the tested frequency is about 11.1 Hz and w_n is about 69.78 rad/s.

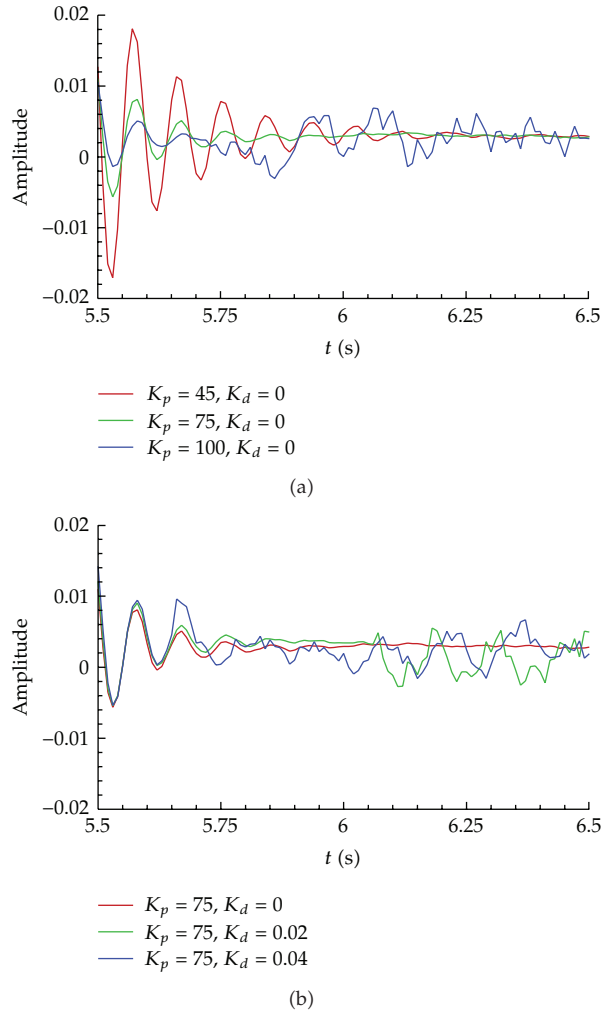

Figure 5: Effect of PID factors on control results.

4.2. PID Control

PID controller is the kind of controller of which proportional gain and derivative gain can be determined based on desired specifications and dynamics of a plant. The optimized parameter adjusted PID controller is widely used in vibration suppression. The turning process can be obtained from an optimal PID control procedure. PID factors play important roles in the control effect in this experiment setting. As shown in Figure 5(a), for a given $K_d = 0$, the best K_p is 75. However, K_d also plays an important role. From Figure 5(b), once $K_d \geq 0.02$, the control effect becomes worse even the K_p is taken as 75. Therefore, the optimal combination of PID factors is required to obtain the best control result.

To determine the optimal factors combination, totally 36 different combinations of K_p and K_d were tested in the experiment, that is, $K_p = 5, 15, 25, 35, 45, 55, 65, 75$, and 100, $K_d = 0$, 0.02, 0.04 and 0.06. In all cases, the K_i is chosen as $K_i = 8$. To evaluate the control effect, the

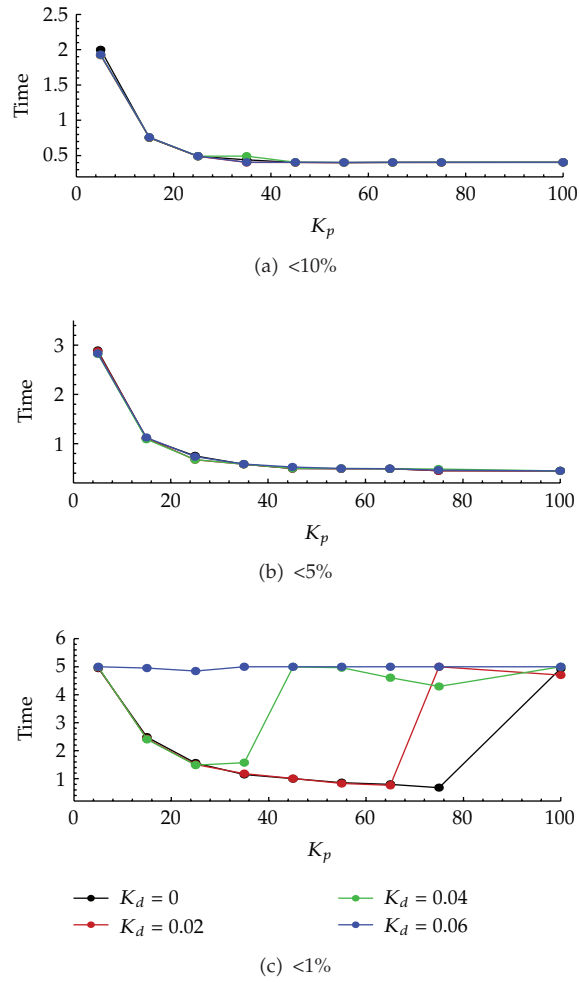

Figure 6: Vibration damping time associated with K_p and K_d combination. (a) vibration damping 90%; (b) vibration damping 95%; (c) vibration damping 99%.

Table 1: Comparison of time for amplitude damping 99% between different K_p and K_d combinations.

K_d	K_p								
	5	15	25	35	45	55	65	75	100
0	4.952	2.483	1.560	1.151	1.001	0.857	0.799	0.681	4.936
0.02	4.972	2.427	1.509	1.181	1.006	0.829	0.766	4.999	4.704
0.04	4.988	2.404	1.485	1.573	4.994	4.965	4.608	4.294	4.999
0.06	4.998	4.953	4.846	4.999	4.998	4.999	4.998	4.999	4.999

time required for amplitude damping 99% is employed to compare control capability. Table 1 presents the control effect comparison between different K_p and K_d combinations.

The test results indicate, the best optimal combination of K_p and K_d depends on how good we want the final vibration damping. Referring to Figure 6, apparently, if the threshold of "vibration damping" is 10% or 5% of the initial maximum amplitude, the vibration

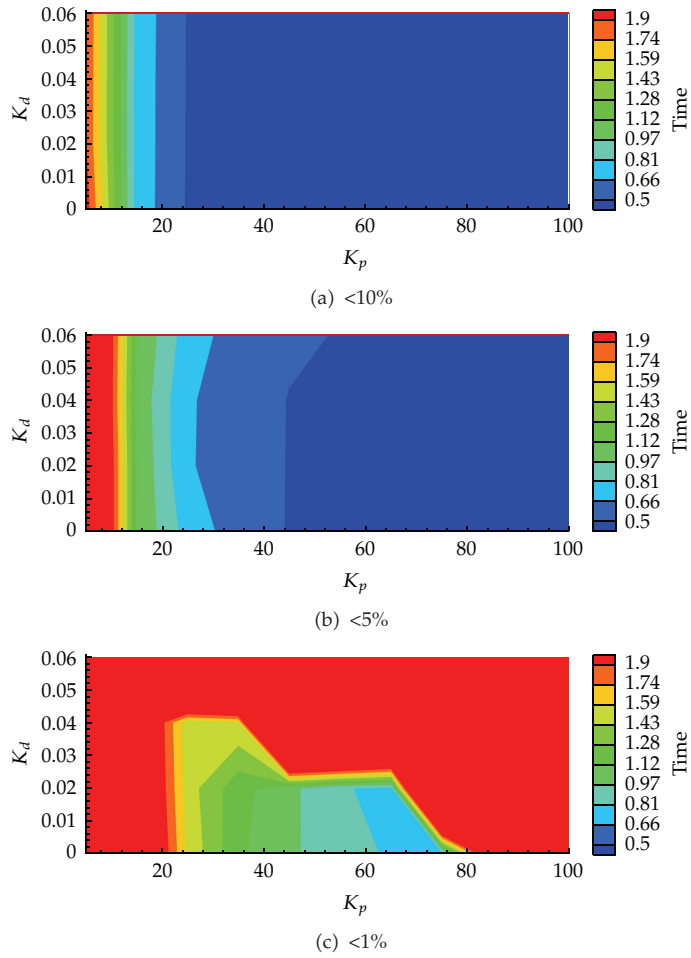

Figure 7: Contour plots of vibration damping time associated with K_p and K_d. (a) vibration damping 90%; (b) vibration damping 95%; (c) vibration damping 99%.

damping time decreases as increasing K_p and almost keep constant after $K_p = 50$ while the influence of K_d is very tiny. However, if the threshold is 1%, K_d has some special influence. For each value of K_d, PID control could reach 99% damping under some certain value of K_p. For example, when K_d is 0.02, K_p is about 75. When $K_d = 0.04$, K_p is about 30. It can be derived from Figure 6(c) that the value of optimal K_p increases with respect to the decreasing K_d.

To better give a look, several contour figures were presented in Figure 7. The contour value is the time for vibration damping 90%, 95% and 99% respectively. Figure 7 obviously indicates that, under this experimental settings, the best combination of K_p and K_d locates at $0 \leq K_d \leq 0.02$ (as shown in Figure 7(c)).

K_p and K_d are two major parameters to control the PID control mechanism. The test results indicate, the best optimal combination of K_p and K_d depends on how good we want the final vibration damping. Generally speaking, K_p has the dominant influence while K_d has to be selected carefully.

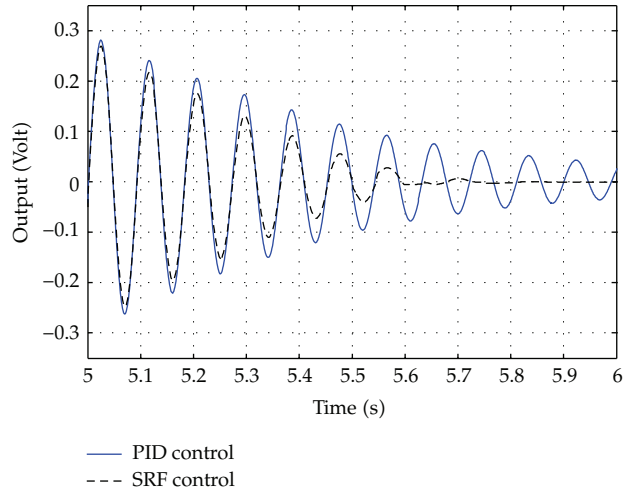

Figure 8: Experimental comparison of SRF control and PID control.

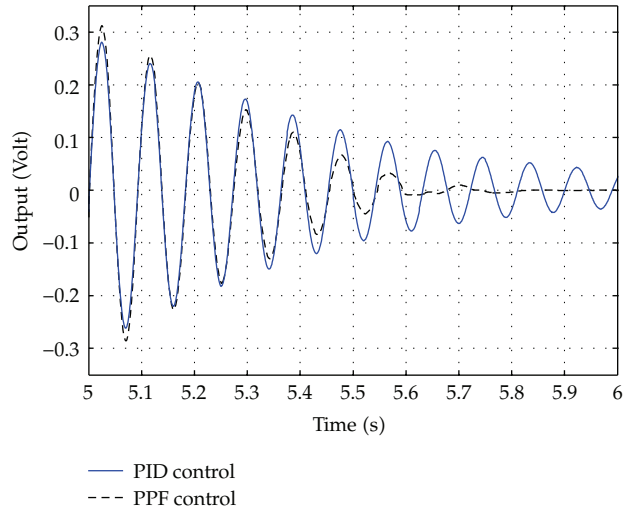

Figure 9: Experimental comparison of PPF control and PID control.

4.3. SRF and PPF Control

The strain rate feedback control was implemented in real time on the beam using the xPC Target system. The same low pass filter is used as in PID experiment. The mode targeted for control was the dominant frequency of 11.1 Hz. The SRF-controller-damping ratio ζ_c was set at 0.5, controller frequency ω_c was set at 11.1 Hz which was set to the vibration frequency of the normal specimen, and the effectiveness of the SRF-controller at various gains was tested. The controller gain K was adjusted to be 1.1 for the consideration of maximum applicable voltage and optimal vibration suppression result. The beam was excited by a sinusoidal signal for 5 s in both the cases of uncontrolled and controlled vibrations. The SRF-controlled time response compared with PID control is depicted in Figure 8. The PPF controlled

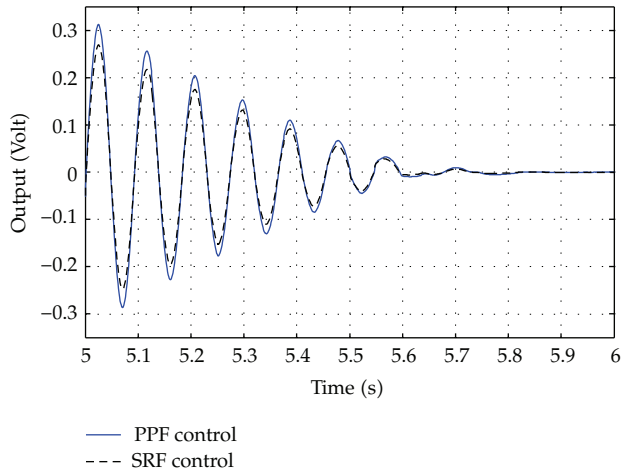

Figure 10: Experimental comparison of SRF control and PPF control.

time response compared with PID control is depicted in Figure 9. The SRF-controlled time response compared with PPF control is depicted in Figure 10. The experimental results successfully demonstrated the vibration suppression of a steel cantilever steel beam using SRF and PPF control. Moreover, SRF control is better than PPF control for this experiment. Both SRF and PPF control have better vibration suppression result for the beam compared with PID control. The PPF was by far the most effective control strategy; however, it is accompanied with initial overshoot. SRF results were better than those with the PPF and PID controllers, but the maximum damping was limited, as the system tends to be unstable at higher gains. Design of the PPF and SRF-controller requires that the natural frequency of the structure to be known exactly and not to vary with time, because the performance of the PPF and SRF-controller will be adversely affected if it was different.

5. Conclusion

The optimal PID control, SRF and PPF controller are employed to actively suppress vibration of a flexible steel cantilever beam. Suppression of the single dominant mode vibration is carried out and the best result is obtained using SRF-controller. The optimal PID controller and PPF controller are also effective in suppressing the vibration. Experimental results successfully demonstrated the effectiveness of vibration suppression using the optimal PID controller, SRF and PPF controllers.

Acknowledgments

This work was supported by National Science Foundation of China under Grant No. 61074056, The Natural Science Foundation of Jiangsu Province under Grant no. BK2010201. The authors thank to the anonymous reviewer for useful comments that improved the quality of the paper. The assistance and support from Dr. Z. Li, Dr. S. Hua, and Professor Steven Seelecke from North Carolina State University are appreciated.

References

[1] S. M. Newman, *Active damping control of a flexible space structure using piezoelectric sensors and actuators*, M.S. thesis, U.S. Naval Postgraduate School, 1992.

[2] E. F. Crawley and J. de Luis, "Use of piezoelectric actuators as elements of intelligent structures," *AIAA journal*, vol. 25, no. 10, pp. 1373–1385, 1987.

[3] J. L. Fanson and T. K. Caughey, "Positive position feedback control for large space structures," *AIAA Journal*, vol. 28, no. 4, pp. 717–724, 1990.

[4] G. Song, P. Qiao, V. Sethi, and A. Prasad, "Active vibration control of a smart pultruded fiber-reinforced polymer I-beam," *Smart Materials and Structures*, vol. 13, no. 4, pp. 819–827, 2004.

[5] G. Song, S. P. Schmidt, and B. N. Agrawal, "Active vibration suppression of a flexible structure using smart material and a modular control patch," *Proceedings of the Institution of Mechanical Engineers. Part G*, vol. 214, no. 4, pp. 217–229, 2000.

[6] A. Baz and S. Poh, "Optimal vibration control with modal positive position feedback," *Optimal Control Applications and Methods*, vol. 17, no. 2, pp. 141–149, 1996.

[7] M. I. Friswell and D. J. Inman, "Relationship between positive position feedback and output feedback controllers," *Smart Materials and Structures*, vol. 8, no. 3, pp. 285–291, 1999.

[8] S.-B. Choi and C.-H. Lee, "Force tracking control of a flexible gripper driven by piezoceramic actuators," *Journal of Dynamic Systems, Measurement and Control, Transactions of the ASME*, vol. 119, no. 3, pp. 439–446, 1997.

[9] S. S. Ge, T. H. Lee, and J. Q. Gong, "Dynamic modeling of a smart materials robot," *AIAA Journal*, vol. 36, no. 8, pp. 1466–1478, 1998.

[10] P. Gaudenzi, R. Carbonaro, and E. Benzi, "Control of beam vibrations by means of piezoelectric devices: Theory and experiments," *Composite Structures*, vol. 50, no. 4, pp. 373–379, 2000.

[11] Q. Wang and S. T. Quek, "Flexural vibration analysis of sandwich beam coupled with piezoelectric actuator," *Smart Materials and Structures*, vol. 9, no. 1, pp. 103–109, 2000.

[12] J. Fei and Y. Fang, "Robust adaptive feedforward vibration control for: Flexible structure," *International Journal of Innovative Computing, Information and Control*, vol. 6, no. 5, pp. 2189–2197, 2010.

[13] J. Fei and Y. Fang, "Active feedback vibration suppression of a flexible steel cantilever beam using smart materials," in *Proceedings of the 1st International Conference on Innovative Computing, Information and Control (ICICIC '06)*, pp. 89–92, September 2006.

[14] Y. Jiang, Q. Hu, and G. Ma, "Design of robust adaptive integral variable structure attitude controller with application to flexible spacecraft," *International Journal of Innovative Computing, Information and Control*, vol. 4, no. 9, pp. 2431–2440, 2008.

[15] Z.-C. Qiu, H.-X. Wu, and D. Zhang, "Experimental researches on sliding mode active vibration control of flexible piezoelectric cantilever plate integrated gyroscope," *Thin-Walled Structures*, vol. 47, no. 8-9, pp. 836–846, 2009.